Silicon Substitution in Biphasic Calcium Phosphate Bioceramics: Crystal Structure Study

B. El ouatli, M. Jamil, A. Elouahli, El. Gourri, M. Ezzahmouly, F. Abida, M. Ilou, Z. Hatim
Team of Electrochemistry and Biomaterials, Department of Chemistry, Faculty of Sciences,
University of Chouaib Doukkali, El Jadida, Morocco.

Abstract— Silicon substituted (Si-BCP) and unsubstituted (BCP) biphasic Calcium Phosphate are prepared by solid-solid reaction. The prepared powders are characterized by Fourier Transform Infrared spectroscopy and X-ray Diffraction. The Rietveld refinements are performed with FullProf program. The results show that the SiO_4^{4-} group substitutes the PO_4^{3-} group in two phases: Hydroxyapatite ($Ca_{10}(PO_4)_6(OH)_2$: HAP) and β-Tricalcium phosphate ($Ca_3(PO_4)_2$: β-TCP). In the TCP structure, this substitution induces an increase of parameter (a), a decrease of parameter (c) and a decrease of cell volume. In the HAP lattice, this substitution induces an increase of parameter (c), a decrease of lattice parameter (a) and a decrease of cell volume. The insertion of silicon in the hydroxyapatite structure causes a shift in the position of the oxygen and phosphorus atoms and perturbations at P-O1, P-O2, P-O3, Ca2-O1, Ca2-O2, and Ca2-O3 distances. The substitution of PO_4^{3-} by SiO_4^{4-} group causes also a reduction of the hydroxyl group, an increase in the occupancy rate of all sites and an increase of lattice distortion index (D_{ind} = 6.995) compared to the unsubstituted hydroxyapatite value (D_{ind} =4.782) and to the theoretical value (D_{ind} = 3.079). This structural change increases the dissolution of BCP which enhances the biological activity of these bioceramics.

Index Terms— Bioceramics, Hydroxyapatite, Tricalcium Phosphate, Silicon, Structure study.

1 Introduction

Synthetic hydroxyapatite ($Ca_{10}(PO_4)_6(OH)_2$: HAP, with molar ratio Ca/P = 1,667) has some advantages as a biomaterial due to its structure that is similar to the mineral part of bone and human tissues [1],[2]. For this reason it is used in many medical and dental applications [3]. However, stoichiometric hydroxyapatite is not resorbable in the body and may cause critical problems in orthopedic and dental clinics [4]. The combination of hydroxyapatite with tricalcium phosphate ($Ca_3(PO_4)_2$: β-TCP, molar ratio Ca/P = 1.50), which has high resorbability gives a biphasic mixture HAP/TCP (1.50 < Ca/P <1.667), which combines the physico-chemical properties of the two compounds. [5] Furthermore, hydroxyapatite may be doped with ions to enhance its resorbability. Indeed, ions of calcium might be partially replaced with other identical or different valent ions such as strontium, magnesium, silicon ... [6],[7],[8].

Silicon has been identified as an important element in the chemical composition of bone [9],[10]. The benefit of the addition of silicon in the hydroxyapatite structure is evaluated in vitro and in vivo and greater bioactivity is demonstrated on Si-HAP compared to pure HAP [11], [12], [13]. Osteoblastic cell proliferation studies have shown the biocompatibility of the silicated hydroxyapatite [14], [15]. The high silicon content in HAP leads to a high cell proliferation [12].

There are few studies on the silicon incorporation into the β-tricalcium phosphate structure. However, osteoblastic cell proliferation studies have also shown the biocompatibility of the silicated β-TCP [16],[17].

Various studies dealing with the substitution of phosphate group (PO_4^{3-}) by silicate group (SiO_4^{4-}) in hydroxyapatite structure [12],[14],[18],[19]. The geometry of these two anions and their very similar sizes, do not cause structural problems in hydroxyapatite and in β-tricalcium phosphate. However the difference in charge must be taken into account and a load compensation mechanism must be achieved.

Various methods of synthesis of hydroxyapatite doped with silicon have been proposed as the sol-gel method, hydrothermal synthesis [20], and the aqueous method [21], [22]. The insertion of silicates ion in calcium-hydroxyapatite is also possible by solid-solid reaction [23]. This method generally yields stoichiometric and well crystallized products. However, this preparation requires high temperatures between 1100°C and 1400°C with repeated calcinations cycles.

In this work, we prepared Silicon substituted (Si-BCP) and unsubstituted (BCP) biphasic Calcium Phosphate by solid-solid reaction with single calcination step at 900°C. We studied the incorporation effect of silicon on the structure of hydroxyapatite and tricalcium phosphate phases.

• *Corresponding author: M. Jamil*
E-mail: mo.jamil@yahoo.fr

2 MATERIALS AND METHODS

2.1 Powders preparation

The preparation of biphasic calcium phosphate bioceramics is performed from calcium carbonate ($CaCO_3$: analytical grad), silica (SiO_2: analytical grade) and pure tricalcium phosphate (β-$Ca_3(PO_4)_2$) prepared by solid state reaction. The powders were weighed and mixed with molar ratio Ca/P (BCP) and Ca/(P+Si) (Si-BCP) constant and equal to 1.623 and the used amount of SiO_2 was 1 wt.%. The obtained mixture was ground in ethanol for several hours. For each product the calcinations were carried out at 900 °C for 3 hours. The heating rate is selected from 5 ° C / min to ensure an even heating of the furnace.

2.2 Characterization of powders

2.2.1 Infra-red spectroscopy

The chemical absorption characteristics of heat-treated powders were characterized by Fourier transforms infrared spectroscopy (KBr pellet method, Bio-Rad Win-IR Pro). For this purpose, 1 wt.% of the powder was mixed and ground with 99% of potassium bromide (KBr, 0.2 g). The spectrum was taken in the range of 400–4000 cm^{-1} with resolution 4cm^{-1} and 20 scans.

2.2.2 Rietveld Refinements

X-ray powder data were collected on D5000 operating in step scan mode using Cu radiation. X-ray data were collected between 10° and 90° with a 0.02° 2θ step and counting 15s by step. Rietveld refinements were performed with FullProf code [24]. Refined values (a and c cell parameters, atomic positions, site occupancies, thermal parameters) of stoichiometric hydroxyapatite [25] were used as the starting model. Refined values (a and c cell parameters) of β-TCP [26] were also used as the starting model. The pseudoVoigt function was used to present the individual reflection profiles. In the final step of the refinement, all atomic positions and site occupancies were refined simultaneously with atom displacement factor. In the last cycle of refinement, 33 structural and non-structural parameters were optimized. The tetrahedral distortion index was obtained from the calculated data using the relation (1) [27]:

$$D_{ind} = \frac{\sum_{i=1}^{6}(OPO_i - OPO_m)^2}{6} \quad (1)$$

Where OPO_i denotes the six angles between P and the four O atoms of the phosphate tetrahedron and OPO_m is the average angle (around 109.17°).

The Rc factor is calculated using equation (2):

$$R_c = \frac{d(Ca2 - Ca2)}{2} tan\frac{\pi}{6} \quad (2)$$

Where d(Ca2 - Ca2) represents the length of the bond Ca - Ca.

3 RESULTS AND DISCUSSION

3.1 Powders characterization

XRD patterns record for the prepared samples BCP and Si-BCP are shown in Fig. 1. The results indicate: i) the samples are composed of the crystallized HAP and β-TCP phases while the α-TCP and SiO_2 phases are absent. This result indicates that the reaction between β-TCP, $CaCO_3$ and SiO_2 is total and in agreement with the literature the absence of α-TCP indicates a relatively low silicon substitution in the TCP phase. ii) Unsubstituted powder from BCP presents an amount of β-TCP less than that Si-BCP contains. The amount of β-TCP depends on the silicon substitution; this amount of β-TCP increases with the increase of silicon amount [28].

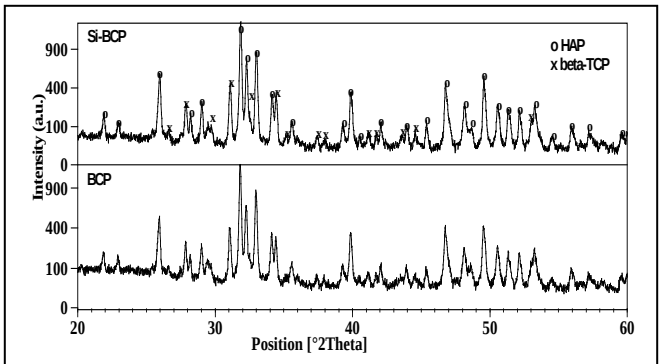

Fig.1. XRD patterns of prepared BCP and Si-BCP.

Fig. 2 shows the infrared spectra of the samples BCP and Si-BCP. The bands at 3574 cm^{-1} and 633 cm^{-1} corresponds to hydroxyl group stretching and vibrational modes, respectively. The intense bands at 962 cm^{-1} corresponds to P-O stretching vibration modes, while the doublet at 603-569 cm^{-1} corresponds to bending O-P-O mode. In addition, the broad band at 3468 cm^{-1} is attributed to the moisture in the samples. The same four fundamental vibration modes are found in the SiO_4^{4-} group, with frequencies rather near to those of the PO_4^{3-} vibrations, therefore it is quite difficult to discriminate between them [29]. In our case, we have a very low content of Silicon (1 wt. %) which explains the absence of the absorption band of SiO_4 group.

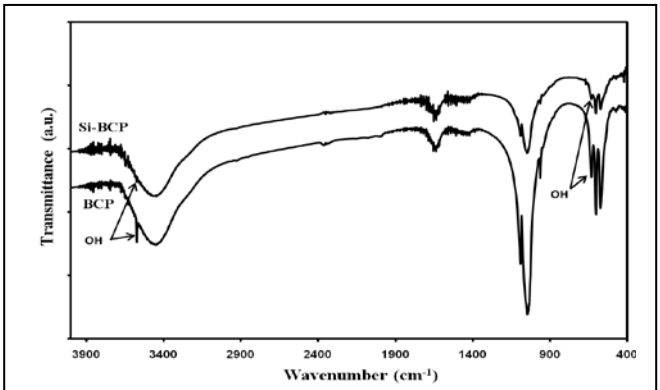

Fig.2. FTIR spectra of prepared BCP and Si-BCP

The significant effect of the silicon addition was the decrease in the hydroxyl stretching bands at 3571 cm^{-1} and 631 cm^{-1} and phosphate stretching bands at 965 cm^{-1}. This can be related to the substitution of PO_4^{3-} by SiO_4^{4-} tetrahedrons, within the hydroxyapatite structure. The incorporation of silicon ion in the hydroxyapatite phase induces a reduction of the amount of hydroxyl groups to compensate for the extra negative charge of the silicates group. The (s) proposed mechanism to explain these structural changes can be described by the following reaction (3):

$$PO_4^{3-} + OH^- \quad \leftrightarrow \quad SiO_4^{4-} + \square OH \qquad (3)$$

(□OH indicates a vacancy in the hydroxyl site)

3.2 Rietveld Refinements

The structural refinements of the BCP and Si-BCP were performed using the FullProf program (2012). Fig. 3 shows the result of the Refinements (Y calculated) the diffractogram of the powder (Y observed) and the difference between these two diagrams. This figure reflects the good fit between the refined function and the values measured experimentally. The good agreement between observed and calculated data is indicated by the low values of chi2 factors (chi2(BCP)= 2.123, chi2(Si-BCP)= 2.353).

The volume and the lattice parameters of the HAP and TCP phases are given in Table 1. The results show that the substitution of PO_4 by SiO_4 group in the hydroxyapatite structure induces a decrease of the cell volume, a decrease of the lattice parameter a-axis, and an increase of the following lattice parameter c-axis. Variations in the lattice parameters (a-c) and the cell volume from different previous studies are heterogeneous [30]. The results of this work are in accordance with the work of Gibson et al [18]. On the other hand, the substitution of PO_4 by SiO_4 group in the TCP structure induces an increase of parameter (a) and a decrease of the parameter (c) and a decrease of cell volume (table 1). These structural changes in the sample Si- BCP show that the SiO_4 group substitutes the PO_4 group in two phases HAP and TCP.

The substitution in β-TCP phase can be described by the following formula: $Ca_{(3-x)}\ (PO_4)_{(2-2x)}\ (SiO_4)_x$. This structure induces a reduction of the amount of calcium ion to compensate the extra negative charge, which leads to a contraction of the lattice. This structural change could explain the evolution decrease in lattice parameters (c) and volume cell of β-TCP.

On the other hand, the calcium phosphate structure shows that the PO_4 groups are surrounded by calcium ions. The global charge of the SiO_4 group is -4 when it is -3 for the PO_4 group. This difference in the charges leads to the generation of Colombian force by the silicate on the calcium cation, and is greater than that produced by the phosphate. Indeed, the Colombian force $F_{1/2}$ exerted by an electric charge q1, placed at the point of radius vector r1, on a charge q2 placed at point of radius vector r2, is defined according to equation (4), where ε_0 is the permittivity of vacuum ($\varepsilon_0 \sim 8{,}854.10^{-12}$ $F.m^{-1}$). These phenomena could also explain the evolution of measured lattice parameters and volume cell.

$$\vec{F}_{1/2} = \frac{q_1 q_2}{4\pi\varepsilon_0} \frac{\vec{r}_2 - \vec{r}_1}{|\vec{r}_2 - \vec{r}_1|^3} \qquad (4)$$

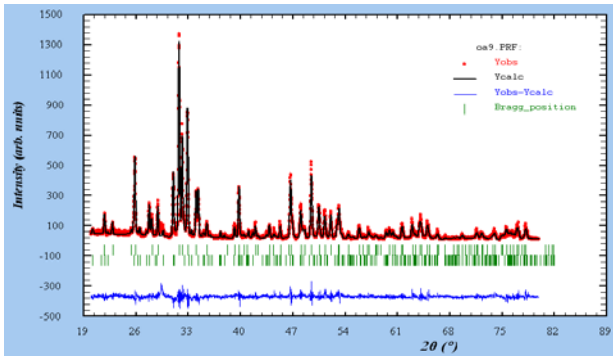

Fig.3. X-ray diffraction pattern of prepared Si-BCP powder (___ experimental ** calculated).

Table 1 Calculated lattice parameters and cell volume of HAP and TCP in BCP and Si-BCP.

Sample	a (Å)	b (Å)	c (Å)	V(Å³)
HAP (BCP)	9.4198	9.4198	6.8805	528.73
HAP(Si-BCP)	9.4170	9.4170	6.8820	528.56
TCP(BCP)	10.4319	10.4319	37.4222	3526.84
TCP(Si-BCP)	10.4335	10.4335	37.3954	3525.42

The interatomic distances and the angles OPO for HAP phase are given in table 2. The insertion of silicon causes a shift in the position of the oxygen and phosphorus atoms (table 3) and perturbations at the distances P-O(1), P-O(2), P-O(3), Ca(2)-O (1), Ca (2) -O (2), and Ca(2)-O (3). We note an increase of the distance P–O(3) and Ca(2)-O(3)with a slight decrease in the distance Ca(2)–O(3) and Ca(2)-O(2). The OPO angles are also affected: a decrease of O(1) -P- O(2), O(1) -P-O(3) angles and an increase of O(2) -P- O(3), O(3) -P- O(3) angles (table 2). These perturbations causes a greater distortion in the tetrahedron PO_4 (D_{ind} (Si-BCP) = 6.9953) than those of the HAP in BCP (D_{ind} (BCP) = 4.7817) and the theoretical hydroxyapatite value (D_{ind} = 3.079).The calculated value of Rc factor (Rc(BCP)= 1.1867 ; Rc(Si-BCP)= 1.1876) confirms the tunnel perturbation.

The atomic coordinates and equivalent isotropic displacement parameters of HAP in BCP and Si-BCP samples

are given in Table 3. The increase of the values of rate occupancy of all site accompanied by decrease of BISO factor values (Table 2), confirms the insertion of silicon in the HAP structure. The Rietveld analysis conducted on the occupancy rates of the different sites of HAP ions were used to verify the possible mechanisms of substitution of phosphate anions by silicate anions. Indeed, the increase in Ca and O populations is explained by the mechanism (5) and (6), which is compatible with the variations of BISO factor (Table 3).

$$\square_{Ca} + 2PO_4^{3-} \leftrightarrow Ca^{2+} + 2SiO_4^{4-} \quad (5)$$

$$\square_{Ca} + PO_4^{3-} + OH^- \leftrightarrow Ca^{2+} + SiO_4^{4-} + O^{2-} \quad (6)$$

($\square_{Ca}$ indicates a vacancy in Ca^{2+})

The substitution of phosphate group with silicate group and the ability of oxygen ions to substitute the hydroxyl sites lead to a distortion of the hexagonal symmetry. Some authors have described that the fast dissolution of Si-hydroxyapatite is due to the migration to the positioning of whether the grain boundary [31], and a smaller grain size with more triple-junctions per unit area, facilitating increased dissolution at the surface [32],[33]. The results of this work show that the substitution of PO_4^{3-} by SiO_4^{4-} groups leads also to the structural rearrangement in TCP and HAP, the formation of OH site vacancies and distortion of hexagonal hydroxyapatite structure. Therefore, this structural change promotes the dissolution of doped bioceramics. The result of the dissolution study was already discussed in previous study [34].

Table 2 Interatomic distances and angles for HAP phase

	HAP(BCP)	HAP(Si-BCP)	HAP(THE)
P–O(1)	1.556(2)	1.534(8)	1.540(7)
P–O(2)	1.532(1)	1.528(3)	1.545(8)
P–O(3)	1.534(8)	1.593(2)	1.515(5)
O(1)–P–O(2)	111.8(2)	110.0(2)	111.4(6)
O(1)–P–O(3)*2	110.7(1)	108.7(6)	111.1(7)
O(2)–P–O(3)*2	106.4(9)	107.1(6)	109.3(7)
O(3)–P–O(3)	110.7(7)	114.9(0)	106.9(4)
Ca(1)–O(1)	2.425(1)	2.444(9)	2.401(8)
Ca(1)–O(2)	2.415(1)	2.420(2)	2.458(7)
Ca(1)–O(3)	2.794(1)	2.796(7)	2.809(5)
Ca(2)–O(3)	2.319(8)	2.241(7)	2.342(5)
Ca(2)–O(2)	2.401(1)	2.348(5)	2.349(8)
Ca(2)–OH	2.405(7)	2.413(4)	2.382(4)
Ca(2)–O(3)	2.528(1)	2.570(5)	2.514(5)
Ca(2)–O(1)	2.682(2)	2.736(6)	2.708(6)

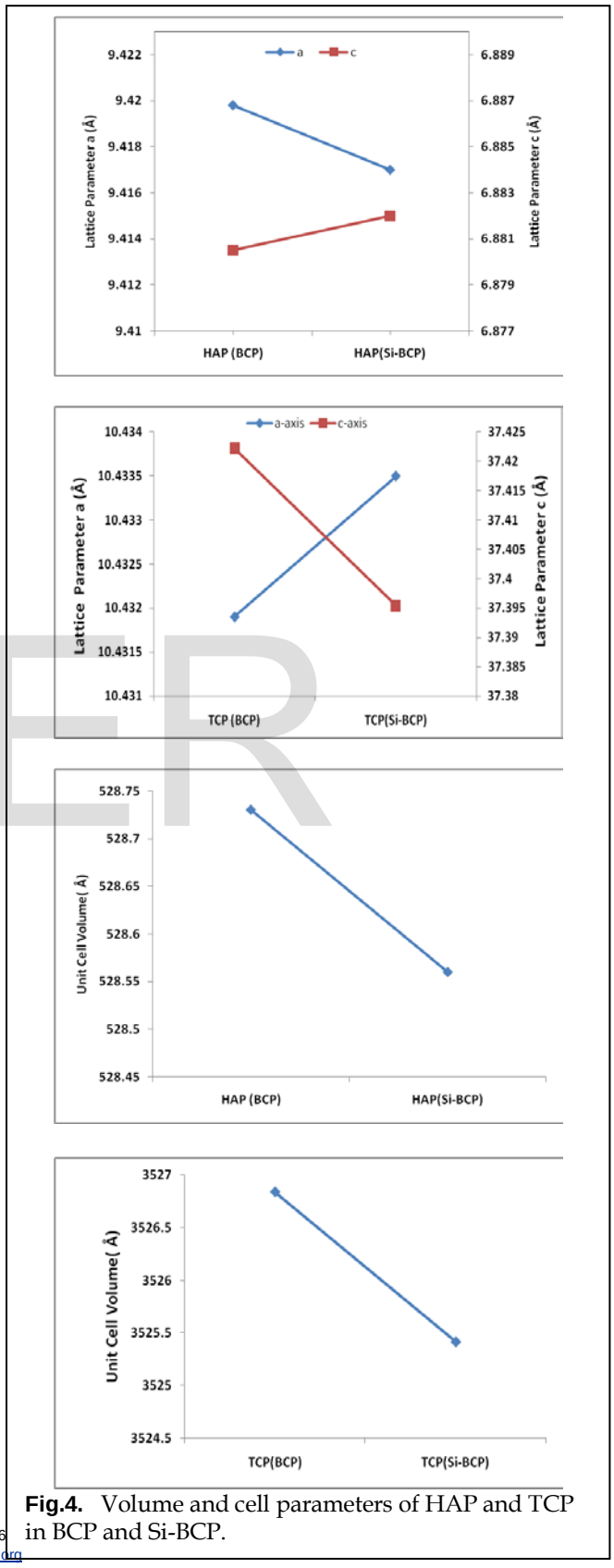

Fig.4. Volume and cell parameters of HAP and TCP in BCP and Si-BCP.

Table 3 Atomic coordinates and equivalent isotropic displacement parameters of HAP.

Atom	Chem	HAP(BCP)						HAP(Si-BCP)					
		x/a	y/b	z/c	Biso	Occ	Mult	x/a	y/b	z/c	Biso	Occ	Mult
Ca1	Ca	0.3333	0.6667	-0.0019	1.8592	0.2940	4	0.3333	0.6667	-0.0041	1.5045	0.3374	4
Ca2	Ca	0.2470	0.9929	0.2500	1.5835	0.4380	6	0.2499	0.9961	0.2500	1.0532	0.4923	6
P	P	0.3968	0.3652	0.2500	1.5004	0.4260	6	0.3984	0.3659	0.2500	1.1298	0.5000	6
O1	O	0.3259	0.4831	0.2500	1.5194	0.4330	6	0.3305	0.4839	0.2500	1.1350	0.4914	6
O2	O	0.5846	0.4591	0.2500	1.8041	0.4710	6	0.5858	0.4628	0.2500	1.5220	0.4773	6
O3	O	0.3436	0.2582	0.0666	1.4808	0.9500	12	0.3426	0.2609	0.0549	1.0000	1.0000	12
O4	O	0.0000	0.0000	0.1830	1.0000	0.1666	2	0.0000	0.0000	0.1850	1.0000	0.1666	2
H	H	0.0000	0.0000	0.0608	1.0000	0.1666	2	0.0000	0.0000	0.0608	1.0000	0.1666	2

4 Conclusion

Silicon substitution in biphasic calcium phosphate (Hydroxyapatite/Tricalcium phosphate) was studied. The samples were prepared by solid-solid reaction at low temperature and with single calcination step. The structural refinements were performed using the FullProf program. The result indicates that the silicon is replacing the phosphate group in the HAP and in the TCP phase, the substitution affects the structural rearrangement in two phases. The insertion of silicon in the hydroxyapatite structure causes higher lattice distortion (D_{ind} = 6.995) compared with the value of the reference HAP (D_{ind} = 4.782) and with the theoretical value (D_{ind} = 3.079 Å). It is assumed that the rearrangement of the structure must change the biological properties, such as solubility and reactivity, of these biomaterials.

References

[1] L.L. Hench, J. Am. Ceram. Soc. 74 (1991) 1487–1510.
[2] S. H. Maxian, J. P. Zawaddsky and M. G. Dunn: J. Biomed. Mater. RES. 28 (1994) 1311.
[3] E. L. Solla, J. P. Borrajo, P. Gonsalez, J. Serra, S. Chiussi, B. Leon and J. Garcia Lopez : Appl. Surf. Sci. 253 (2007) 8282.
[4] M. Mastrogiacoma, A. Muraglia, V. Komlev, F. Peryin, F. Rustichelli, A. Crovace, et al, Orthod. Craniofacial. Res. 8 (2005) 277-284.
[5] S. Yamada, D. Heymann, J-M. Bouler, G. Daculsi. Biomaterials; 18 (1997) 1037–41.
[6] W. Zhang et al. Acta Biomater. 7 (2011)800–8
[7] D. Laurencin et al. Biomaterials 32 (2011)1826–37
[8] Mickaël Palard, Eric Champion, Sylvie Foucaud. Journal of Solid State Chemistry 181 (2008) 1950– 1960
[9] Carlisle, E. M. Science (1970), 167, 179.
[10] Carlisle, E. M. Calc. Tissue Int. (1981), 33, 27.
[11] F. Balas, J. Perez-Pariente, M. Vallet-Regi Journal of Biomedical Materials Research - Part A 66A(2) (2003) 364-375.
[12] M. Vallet-Regi, D. Arcos. Journal of Materials Chemistry 15(15) (2005). 1509-1516.
[13] H. M. d. Silva, M. Mateescu, A. Ponche, C. Damia, E. Champion, G. Soares, K. Anselme. Colloids and Surfaces B: Biointerfaces 75(1) (2010)349-355.
[14] E. S. Thian, J. Huang, M. E. Vickers, S. M. Best, Z. H. Barber, W. Bonfield. Journal of Materials Science 41(3) (2006) 709-717.
[15] M. Palard, J. Combes, E. Champion, S. Foucaud, A. Rattner. D. Bernache-Assollant. Acta Biomaterialia 5(4) (2009) 1223-1232.
[16] A.Bandyopadhyay, S. Bernard, W. Xue, S. Bose. Journal of the American Ceramic Society 89(9) (2006) 2675-2688.
[17] E. S. Ghaith, T. Kasuga, M. Nogami. Key Engineering Materials 309-311 II (2006) 779-782.
[18] I. R. Gibson, S. M. Best, W. Bonfield. Journal of Biomedical Materials Research 44(4) (1999) 422-428.
[19] D. Arcos, J. Rodrìguez-Carvajal, M. Vallet-Regi. Chemistry of Materials 16(11) (2004) 2300-2308.
[20] X.L. Tang, X.F. Xiao, R.F. Liu, Mater. Lett. 59 (2005) 3841–3846.
[21] A. Ruys, J. Aust. Ceram. Soc. 29 (1993) 71–80.
[22] D. Arcos, J. Rodriguez Carvajal,M. Vallet-Regi, Chem.Mater. 16 (2004) 2300–2308.
[23] L. Boyer, J. Carpena, J. Lacout, Sol. State Ionics 95 (1997) 121–129.
[24] J. Rodriguez-Carvajal. Physica B, 192 (1993) 55-69.
[25] K. Sudarsanan, R.A. Young. Acta Crystallographica B, 25 (1969) 1534- 1543.
[26] M. Yashima, A. Sakai, T. Kamiyama, A. Hoshikawa, Journal of Solid State Chemistry 175 (2) (2003) 272–277.
[27] L. J. Jha, S.M.Best, J.C.Knowles, I.Rehman, J.D.Santos and W. Bonfield, J. Mater Sci: Mater. Med. 8 (1997) 185 -191.
[28] S. Gomes, G. Renaudin, A. Mesbah, E. Jallot, C. Bonhomme, F. Babonneau, J.-M. Nedelec. Acta Biomaterialia 6 (2010) 3264–3274
[29] Gheorghe Tomoaia, Aurora Mocanu, Ioan Vida-Simiti, Nicolae Jumate, Liviu-Dorel Bobos, Olga Soritau, Maria Tomoaia-Cotisel. Materials Science and Engineering C 37 (2014) 37–47.
[30] S. Gomes, G. Renaudin, A. Mesbah, E. Jallot, C. Bonhomme, F. Babonneau, J.-M. Nedelec. Acta Biomaterialia 6 (2010) 3264–3274
[31] Alexandra E. Porter, Claudia M. Botelho, Maria A. Lopes, Jose ´ D. Santos, Serena M. Best, William Bonfield. J Biomed Mater Res (2004) 69A: 670–679.
[32] A.E Porter, N. Patel, J.N. Skepper, S.M. Best, W. Bonfield. Biomaterials 24 (2003) 4609–4620
[33] AE. Porter. Micron 37 (2006) 681–688.
[34] M. Jamil, B. El ouatli, A. Elouahli, F. Abida, Z. Hatim, IJSER 7(1) (2016) 593-597.